Journal of Inorganic and General Chemistry
ZAAC
Zeitschrift für anorganische und allgemeine Chemie
www.zaac.wiley-vch.de
RESEARCH ARTICLE

DOI: 10.1002/zaac.202200365

Special Collection

Copper(I) and Gold(I) Complexes of Aminofunctionalized Phosphinines: Synthesis and Structural Characterization

Jinxiong Lin,[a] Daniel S. Frost,[a] Nathan T. Coles,[a, b] Manuela Weber,[a] and Christian Müller*[a]

Dedicated to Prof. Dr. Sjoerd Harder on the occasion of his 60th birthday

A series of novel 3-*N*,*N*-dimethylaminofunctionalized phosphinines were synthesized and structurally characterized. DFT calculations showed that these aromatic phosphorus heterocycles possess stronger π-donor and σ-donor properties compared to the parent phosphinine C_5H_5P. With $CuBr{\cdot}SMe_2$, the corresponding complexes of the type $[(phosphinine)_2CuBr]_2$ are formed, which show the classical terminal σ-coordination mode of the phosphorus donor towards the Cu(I) center. Upon reaction with $AuCl{\cdot}SMe_2$, mononuclear phosphinine-Au(I)Cl complexes could be obtained and crystallographically characterized. Moreover, the presence of a $SiMe_3$-group and a donor-functionality provide the possibility for post-synthetic ligand modifications. With $CuCl{\cdot}SMe_2$ the phosphinine-based hydrochloride salts forms a rare Cu(I) complex with a Cu_4Cl_4-core, that contains two pairs of differently coordinating phosphinine ligands.

Introduction

Phosphinines (phosphabenzenes, phosphorines), the higher homologues of pyridines, are usually regarded as strong π-acceptors and relatively weak σ-donor ligands once coordinated to a metal center. In fact, their electronic properties are especially suited for coordination to late transition metals in low oxidation states.[1] To date, several synthetic routes for the preparation of phosphinines have been reported in the literature. Some of them allow the introduction of functional substituents into specific positions of the 6-membered aromatic heterocycle, which is important for the modification of their stereoelectronic ligand properties and coordination abilities.[2–7]

Recently, we have shown that the basicity and nucleophilicity of the phosphorus lone-pair can be significantly enhanced by introducing σ-donating substituents into the 2-position of the phosphinine ring.[8] This, together with steric factors, can also drastically affect their coordination behaviour towards metal fragments. For instance, the reaction of the parent phosphinine C_5H_5P with $CuBr{\cdot}SMe_2$ leads to the infinite CuBr coordination polymer **A**, which consists of repeating $[(C_5H_5P)_2CuBr]$ units (Figure 1).[8a] The 2-$SiMe_3$-phosphinine, on the other hand, forms the bromido-bridged dimer **B** of the type $[(L)_2CuBr]_2$ upon reaction with $CuBr{\cdot}SMe_2$.[8a] Mathey and co-workers investigated the reaction of a phosphinin-2-ol with CuCl, where they observed the formation of the dimeric Cu(I) complex **C**. This complex contains two σ-P coordinating as well as two μ_2-P-coordinating phosphinines.[9] The corresponding anionic phosphinin-2-olate, reported by Grützmacher and co-workers, acts as a $4e^-$ donor and bridges a cationic $[Au(PPh_3)]^+$ as well as a neutral [AuCl] fragment (**D**).[10] More recently, our group synthesized a neutral 2-*N*,*N*-dimethylamino-substituted phosphinine.[11] The strong interaction between the lone-pair of the nitrogen atom of the NMe_2 group and the aromatic system results in a high π-density at the phosphorus atom. As a

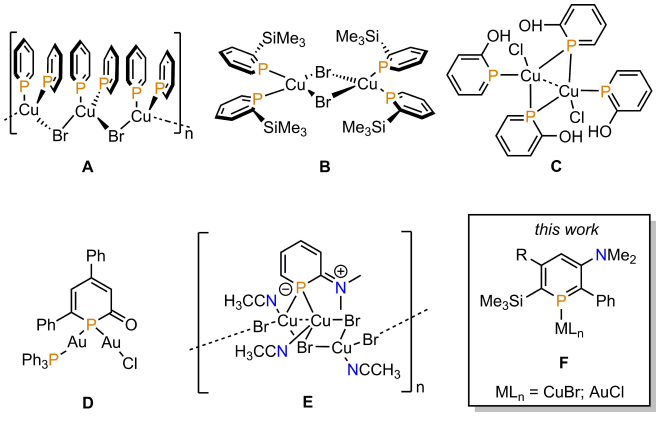

Figure 1. Coordination compounds **A**-**F** of C_5H_5P and various substituted phosphinines and a brief outline of this work.

[a] J. Lin, Dr. D. S. Frost, Dr. N. T. Coles, M. Weber, Prof. Dr. C. Müller
Institut für Chemie und Biochemie
Freie Universität Berlin
Fabeckstr. 34/36, 14195 Berlin (Germany)
E-mail: c.mueller@fu-berlin.de
[b] Dr. N. T. Coles
School of Chemistry
University of Nottingham
University Park Campus, NG7 2RD Nottingham, (UK)

Supporting information for this article is available on the WWW under https://doi.org/10.1002/zaac.202200365

This article is part of a Special Collection dedicated to Professor Sjoerd Harder on the occasion of his 60th birthday. Please see our homepage for more articles in the collection.

consequence, the phosphorus-containing derivative of *N,N*-dimethylaniline acts again as a μ_2-P ligand and forms the coordination polymer **E** when reacted with $CuBr{\cdot}SMe_2$.

In addition, we have recently reported the synthesis, structural characterization and reactivity of the novel 3-*N,N*-dimethylamino-functionalized phosphinine **6** (Scheme 1).[12] As anticipated, this compound shows only a weak interaction between the nitrogen lone pair and the aromatic phosphorus heterocycle, in contrast to observations made for the 2-*N,N*-dimethylaminophosphinine derivative (*vide supra*). We report here on our first results concerning the coordination chemistry of this donor-functionalized phosphorus heterocycle towards Cu(I) and Au(I) (**F**, Figure 1).

Results and Discussion

The 3-*N,N*-dimethylamino-functionalized phosphinines **5**–**7** were synthesised according to a modified literature procedure described by Mathey and co-workers.[5,6] 1,3,2-diazaphosphinine **1** reacts with 1.2 equiv. of trimethylsilylacetylene derivatives in toluene at $T = 70\,^{\circ}C$ to form the corresponding 1,2-azaphosphinines **2**–**4** (Scheme 1). Their formation was monitored by means of $^{31}P\{^{1}H\}$ NMR spectroscopy. After complete conversion of **1** to **2**–**4**, all volatiles were removed under vacuum to prevent further reaction of the slight excess of trimethylsilylacetylenes and 1,2-azaphosphinines at higher temperatures. Compounds **2**–**4** were redissolved in toluene and then reacted with *N,N*-dimethyl-2-phenylethyn-1-amine at $T = 90\,^{\circ}C$ to the desired phosphinines **5**–**7** (Scheme 1). Compounds **5**–**7** were easily purified by means of column chromatography.

The phosphorus heterocycles **5**–**7** show resonances in the $^{31}P\{^{1}H\}$ NMR spectra at $\delta(ppm) = 238.0$ (**5**, CD_2Cl_2), 244.0 (**6**, CD_2Cl_2) and 245.0 (**7**, CD_2Cl_2), respectively. Interestingly, these values are rather different to the shift observed for 2-*N,N*-dimethylaminosphosphinine ($\delta(ppm) = 127.0$).[11] This indicates that the electronic properties of **5**–**7** vary significantly from its regioisomer. Crystals of **5**–**7**, suitable for X-ray diffraction, were obtained by slow evaporation of the solvent from a solution of the phosphinines in *n*-hexanes. The molecular structure of **5** in the crystal is depicted in Figure 2, along with selected bond lengths and angles (for the crystallographic characterization of **6**, see ref. [12]; for **7** see supporting information).

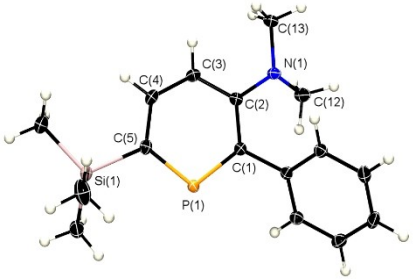

Figure 2. Molecular structure of **5** in the crystal. Displacement ellipsoids are shown at the 50 % probability level. Selected bond lengths [Å] and angles [°]: P(1)–C(1): 1.737(1); P(1)–C(5): 1.731(1); C(5)–C(4): 1.397(2); C(4)–C(3): 1.387(2); C(3)–C(2): 1.407(2); C(2)–C(1): 1.419(2); N(1)–C(2): 1.393(2); C(5)–Si(1): 1.875(1). C(5)–P(1)–C(1): 104.68(5); C(12)–N(1)–C(2): 119.48(9); C(2)–N(1)–C(12)–C(13): 144.9(1).

The crystallographic characterization of **5**–**7** reveal similar C–N bond distances of 1.393(1) (**5**), 1.407(1) (**6**) and 1.415(2) Å (**7**). Moreover, the nitrogen atom of the *N,N*-dimethylamino-substituent is clearly pyramidalized in all three phosphinines. Consequently, we anticipate that the lone pair of the nitrogen atom only weakly contributes in conjugation with the aromatic phosphorus heterocycle, in contrast to the situation for 2-*N,N*-dimethylaminophosphinine.[11]

Having synthesized the novel 3-*N,N*-dimethylamino-substituted phosphinines **5**–**7**, we were further interested in the electronic properties of the ligands, particularly with respect to the parent phosphinine C_5H_5P as well as the 2-*N,N*-dimethylamino-functionalized regioisomer, recently reported by us.[11] As already demonstrated for phosphinine **6**, we also found an area of increased electron density close to the nitrogen atom in the electrostatic potential (ESA) maps of **5** and **7**, suggesting the presence of a lone pair that is not part of the aromatic phosphorus heterocycle (Figure 3).

This effect is clearly caused by the steric demand of the phenyl-group in the 2-position of **5**–**7**. In fact, both the 2-*N,N*-

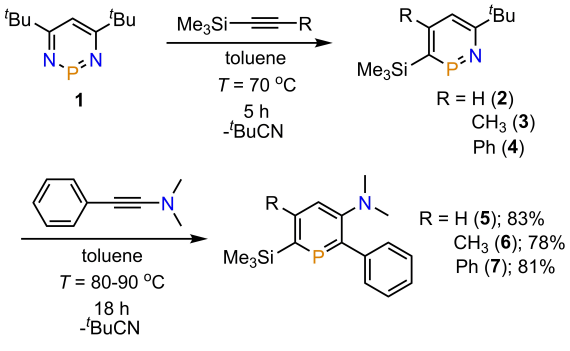

Scheme 1. Synthesis of phosphinines **5**–**7**.

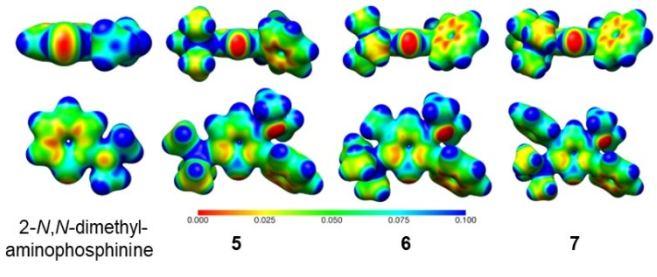

Figure 3. Electrostatic potential maps for 2-*N,N*-dimethylaminophosphinine (left) and phosphinines **5**–**7**. The electrostatic potential (in a.u.), color-coded from 0 (red) to 0.1 (blue), is mapped on electron density isosurfaces of 0.02 e/au^3. The calculations were performed at a B3LYP–D3/def2-TZVP level of theory.[10]

dimethylamino-[11] as well as the 3-*N*,*N*-dimethylamino-substituted phosphinine,[12] without any other substituents at the phosphorus heterocycle, show a fully planar nitrogen atom (Figure 3, left).

Additionally, significant differences can be found in the frontier Kohn-Sham orbitals of the parent phosphinine C_5H_5P, **5** and 2-*N*,*N*-dimethylaminophosphinine (Figure 4).

While the energy of the LUMO for **5** is similar to that of C_5H_5P, both are considerably lower in energy than the LUMO in 2-*N*,*N*-dimethylaminophosphinine. This is in line with the reduced π-acceptor property of this compound, due to the efficient electronic interaction between the nitrogen lone-pair and the aromatic phosphorus heterocycle (*vide supra*). On the other hand, particularly the presence of the $SiMe_3$-group in the 2-position of the ring leads to stronger σ-donor properties of **5**, while the 3-*N*,*N*-dimethylamino-substituent increases the π-donor capability at the same time when compared to the parent phosphinine . However, this is still less than for 2-*N*,*N*-dimethylaminophosphinine due to the strongly reduced interaction of the lone-pair with the phosphorus heterocycle. The fact that the lone-pair in 2-*N*,*N*-dimethylaminophosphinine (HOMO-2) is lower in energy than the one in **5** can be attributed to the electronegative character of the nitrogen atom in close proximity to the phosphorus atom.

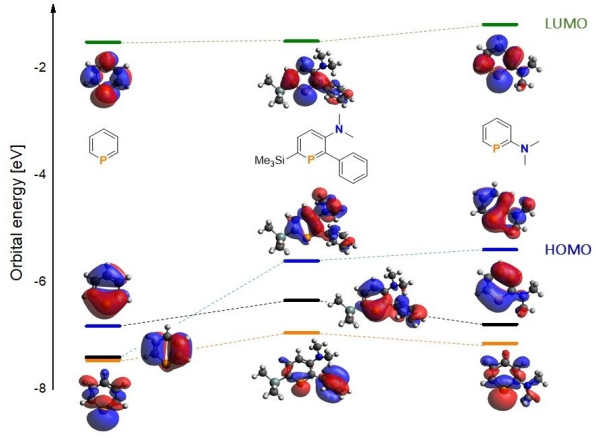

Figure 4. Kohn-Sham orbitals of C_5H_5P (left), **5** (middle) and 2-*N*,*N*-dimethyl-aminophosphinine (right). Energy level of lone pair in orange. The calculations were performed at a B3LYP–D3/def2-TZVP level of theory.[10]

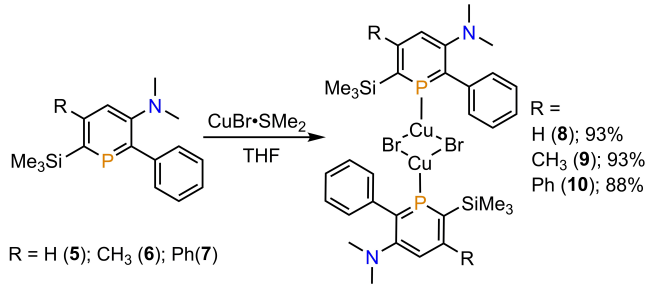

Scheme 2. Synthesis of coordination compounds **8**–**10**.

Having qualitatively elucidated the steric and electronic features of the novel phosphinines, we were further interested in exploring their coordination properties. Phosphinines are known to react readily with Cu(I) precursors to form a variety of different complexes, including infinite stair-like coordination polymers, infinite chain structures, phosphinine-bridged copper dimers as well as tetranuclear heterocubane clusters or polynuclear architectures.[9,13–17] We therefore decided to focus first on the coordination chemistry of the phosphinines towards Cu(I).

Phosphinines **5**–**7** were reacted with $CuBr \cdot S(CH_3)_2$ in THF in a molar ratio of 1:1 (Scheme 2). Only single resonances at δ(ppm) = 202.8, δ(ppm) = 223.0 and δ(ppm) = 224.3 were observed in the corresponding $^{31}P\{^1H\}$ NMR spectra of the reaction mixtures of **8**–**10** after they were stirred overnight at room temperature. The coordination shift difference for **8** of Δδ(ppm) = −35.0 (−21.0 (**9**), −21.0 (**10**)) is indicative of a successful coordination of the phosphinines to Cu(I).

Pale yellow crystals of **8**–**10**, suitable for X-ray diffraction, were obtained by slow evaporation of the solvent from a solution of the coordination compounds in acetonitrile. Complex **8** crystallizes in the triclinic space group *P*-1, while complexes **9** and **10** crystallize in the monoclinic space group $P2_1/c$. The molecular structures of the complexes **8** and **10** in the crystal are depicted in Figures 5 and 6, along with selected bond lengths and angles (for the crystallographic characterization of complex **9**, see supporting information).

The molecular structures of **8**–**10** in the solid state reveal the formation of a bromide-bridged dimer of the type $[(phosphinine)CuBr]_2$. The phosphinines in **8**–**10** show a classical terminal 2e⁻-donation *via* the lone-pair of the phosphorus atom to the respective Cu(I) centers. Interestingly, the Cu(I) atom show a rare distorted trigonal planar coordination environment. To the best of our knowledge, this structural motif has so far never been reported for phosphinine-Cu(I) complexes and can

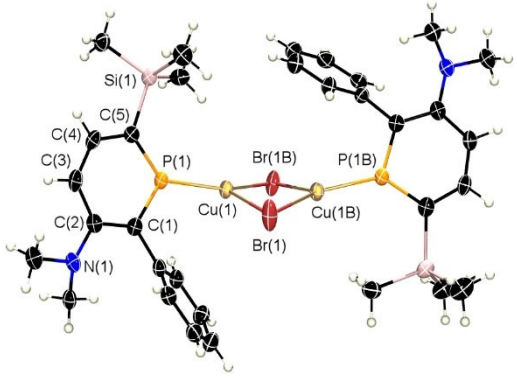

Figure 5. Molecular structure of **8** in the crystal. Displacement ellipsoids are shown at a 50% probability level. Selected bond lengths [Å] and angles [°]: P(1)–C(1): 1.735(4); P(1)–C(5): 1.714(5); Cu(1)–P(1): 2.164(1); Cu(1B)–P(1B): 2.163(1); Br(1B)–Cu(1): 2.3734(9); Br(1)–Cu(1): 2.4142(7); N(1)–C(2): 1.398(6); C(1)–C(2): 1.411(8); C(2)–C(3): 1.413(7); C(3)–C(4): 1.382(7); C(4)–C(5): 1.394(8); C(1)–P(1)–C(5): 108.1(2); Cu(1)–Br(1)–Cu(1B): 76.11(3); Br(1)–Cu(1)–Br(1B): 102.45(3); Cu(1)–Br(1B)–Cu(1B)–Br(1): 12.86(3).

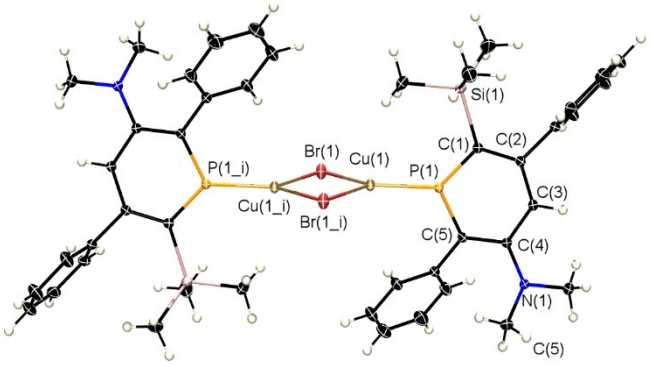

Figure 6. Molecular structure of **10** in the crystal. Displacement ellipsoids are shown at a 50% probability level. The following symmetry operations were used to generate the symmetry equivalent atoms: 1-X, 1-Y, -Z. Selected bond lengths [Å] and angles [°]: P(1)–C(1): 1.724(1); P(1)–C(5): 1.723(1); Cu(1)–P(1): 2.1792(5); Br(1)–Cu(1): 2.4361(4); N(1)–C(4): 1.380(2); C(1)–C(2): 1.416(1); C(2)–C(3): 1.393(2); C(3)–C(4): 1.413(2); C(4)–C(5): 1.421(2). C(1)–P(1)–C(5): 108.42(6); Cu(1)–Br(1)–Cu(1_i): 77.95(1); Br(1)–Cu(1)–Br(1_i): 102.05(1); Cu(1)–Br(1)–Cu(1_i)–P(1_i): 176.33(2).

most likely be rationalized by the steric demand of both the $SiMe_3$- and the Ph-group in 2- and 6-position of the phosphorus heterocycle. In fact, 2-$SiMe_3$-phosphinine forms a dimer of the type $[(phosphinine)_2CuBr]_2$ with $CuBr \cdot S(CH_3)_2$, that shows a distorted tetrahedral coordination environment around the Cu(I) center (**B**, Figure 1).[8a]

Overall, the P–Cu···Cu–P angles increase considerably from 166.07° in **8**, to 170.72° in **9** and 176.05° in **10**. Consequently, the P–Cu_2Br_2–P moiety shows a butterfly-like arrangement in **8**, while it is almost planar in **10** (Figure 5). In contrast to the situation in **E** (Figure 1), containing the 2-*N*,*N*-dimethylaminophosphinine as ligand, the nitrogen atoms in **8**–**10** are clearly pyramidalized, while the C(2)–N(1) bond - lengths (1.407(5) Å (**8**); 1.379(3) Å (**9**), 1.3800(15) Å (**10**)) are considerably longer (**E**: C(2)–N(1): 1.359(8) Å). This indicates a significant C–N single bond character in the phosphinine ligand in **8**–**10**, which is again in line with a strongly reduced interaction of the nitrogen lone-pair with the π-accepting phosphorus heterocycle.

As phosphinines usually react readily with Au(I) precursors, we further investigated the coordination chemistry of **5**–**7** towards $AuCl \cdot S(CH_3)_2$.[18]

The reaction of **5** and **7** with the Au(I) precursor in THF affords a yellow solution (Scheme 3). Unfortunately, under the same reaction conditions, the formation of black particles, which could not be further analyzed, was observed with phosphinine **6** and $AuCl \cdot S(CH_3)_2$. Complexes **11** and **12** show single resonances at δ(ppm) = 193.2 (**11**) and δ(ppm) = 204.7 (**12**) in the corresponding $^{31}P\{^1H\}$ NMR spectra.

Crystals, suitable for X-ray diffraction, were obtained by layering *n*-hexanes onto a solution of complexes **11** and **12** in acetonitrile. The coordination compounds crystallize in the monoclinic space group *Cc* and the triclinic space group *P-1*,

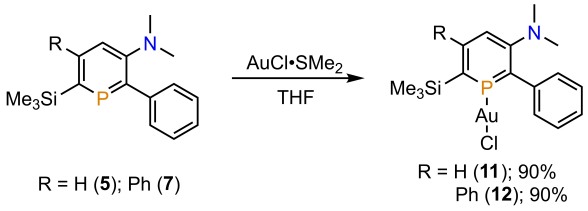

R = H (**5**); Ph (**7**)

R = H (**11**); 90%
Ph (**12**); 90%

Scheme 3. Synthesis of phosphinine-Au(I) complexes **11** and **12**.

respectively. The molecular structure of **11** in the crystal is depicted in Figure 7, along with selected bond lengths and angles (for the crystallographic characterization of **12**: see supporting information).

As expected, both **11** and **12** display an almost linear geometry around the Au(I) center (P(1)–Au(1)–Cl(1): 175.98(5)° for **11**; P(1)–Au(1)–Cl(1): 178.73(3)° for **12**). The phosphorus-Au(I) distances are very similar to the values found for reported phosphinine-AuCl complexes.[17] However, in our case, no aurophilic Au···Au contacts can be found in the unit-cells of **11** and **12**. We anticipate, that the sterically demanding Ph- and $SiMe_3$-substituents in the 2- and 6-position of the heterocyclic ring prevent a close proximity of two coordination compounds to form aurophilic interactions.

Due to the presence of a $SiMe_3$-group and a donor-functionality, we anticipated that the novel phosphinines provide the possibility for post-synthetic ligand modifications.[12] In fact, $SiMe_3$-substituted phosphinines can be protodesiylated, while amino-functionalized phosphinines can be protonated exclusively at the nitrogen-donor.[12,8a,c] Due to the similarity of the here reported phosphorus heterocycles, we focused exclusively on phosphinine **6**. Indeed, the amine functionality in

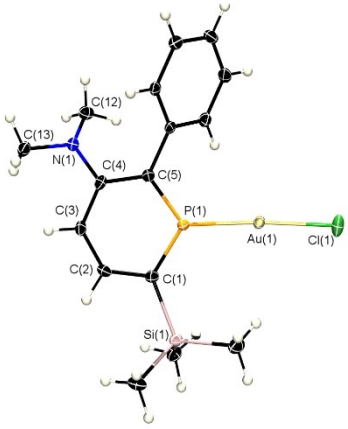

Figure 7. Molecular structure of **11** in the crystal. Displacement ellipsoids are shown at the 50% probability level. Selected bond lengths [Å] and angles [°]: P(1)–C(1): 1.716(5); P(1)–C(5): 1.698(6); C(5)–C(4): 1.396(6); C(4)–C(3): 1.381(8); C(3)–C(2): 1.41(1); C(2)–C(1): 1.426(7); N(1)–C(2): 1.385(7); P(1)–Au(1): 2.213(1); Au(1)–Cl(1): 2.282(1). P(1)–Au(1)–Cl(1): 175.98(5); C(5)–P(1)–C(1): 110.4(2); C(2)–N(1)–C(12)–C(13): 149.9(7).

6 can easily be protonated by adding a slight excess of HCl/Et_2O. Based on the ^1H and ^{31}P NMR spectra, the protonated species **13** is formed quantitatively, with the $SiMe_3$-substituent still located in the *ortho*-position of the heterocycle. The phosphorus resonance of **13** can be found at δ(ppm) = 252.3 in the $^{31}P\{^1H\}$ NMR spectrum. Upon heating **13** in acetonitrile, while excess HCl is still present, protodesilylation occurs, resulting in phosphinine **14**, which shows a signal at δ(ppm) = 212.7 in the $^{31}P\{^1H\}$ NMR spectrum (Scheme 4a). So far, we were not able to isolate any Cu(I)- and Au(I)-complexes when reacting the phosphinine-based hydrochloride salt **14** with $CuBr \cdot SMe_2$ and $AuCl \cdot SMe_2$, respectively.

However, a yellow powder could be obtained in high yield, when reacting **14** with $CuCl \cdot SMe_2$ instead. The $^{31}P\{^1H\}$ NMR shift of the new compound (**15**) occurs at δ(ppm) = 172.8 in THF.

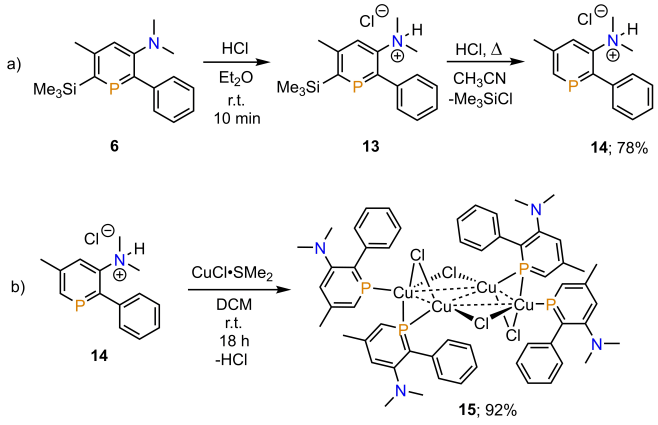

Scheme 4. a) Post-synthesis modification of **6** by protonation and protodesilylation. b) reaction of **14** with a Cu(I) precursor.

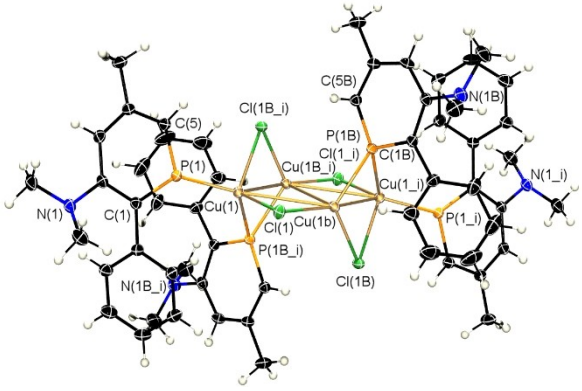

Figure 8. Molecular structure of **15** in the crystal. Displacement ellipsoids are shown at the 50% probability level. The following symmetry operations were used to generate the symmetry equivalent atoms: 1-X, 1-Y, 1-Z. Selected bond lengths [Å] and angles [°]. P(1)–Cu(1): 2.2140(4); P(1B_i)–Cu(1): 2.3469(5); P(1B_i)–Cu(1B_i): 2.2503(4); Cu(1)–Cu(1B_i): 2.4586(4); Cu(1B_i)–Cu(1_i): 3.3433(3); Cu(1)–Cl(1B_i): 2.4157(4); Cu(1B_i)–Cl(1B_i): 2.2758(4); Cu(1B_i)–Cl(1_i): 2.2078(5); Cl(1_i)–Cu(1_i): 2.3334(4). C(1)–P(1)–C(5): 106.14(7); C(5B)–P(1B)–C(1B): 106.32(7).

Crystals of **15**, suitable for single-crystal X-ray diffraction, were obtained from a solution of the complex in a mixture of THF and *n*-hexane at $T = -30\,°C$. Complex **15** crystallizes in the space group *P-1* and the molecular structure of this compound in the solid state is depicted in Figure 8, along with selected bond lengths and angles.

Interestingly, the crystallographic characterization of **15** reveals the presence of a Cu_4-rhombus, which is capped by a total of four chlorido ligands. Additionally, two phosphinine ligands coordinate in the classical σ-coordination mode *via* the phosphorus lone pair to two of the four Cu(I) centers. The other two phosphinine ligands show the rare bridging μ_2-coordination mode and span also two of the four Cu(I) centers (Scheme 4b). To the best of our knowledge, this type of complex is unprecedented in the coordination chemistry of phosphinines so far. As **15** is overall a neutral coordination compound, deprotonation of **14** apparently occurs during complex formation and crystallization.

Conclusions

We have synthesized a series of novel 3-*N*,*N*-dimethylaminophosphinines, starting from 1,3,2-diazaphosphinine, substituted acetylenes and *N*,*N*-dimethyl-2-phenylethyn-1-amine. Based on DFT calculations, the phenyl- and $SiMe_3$-substituents in the donor-functionalized phosphinines increase both the σ-donor and the π-donor capacity of the aromatic heterocycles compared to the parent phosphinine C_5H_5P. However, the increase of π-electron density at the phosphorus atom of the phosphinines is still weaker than in 2-*N*,*N*-dimethylaminophosphinine due to a much weaker interaction between the lone-pair of the exocyclic nitrogen atom and the aromatic phosphorus heterocycle, as shown by the calculated electrostatic potential maps. The 3-*N*,*N*-dimethylaminophosphinines readily react with $CuBr \cdot SMe_2$ to form bromide-bridged dimers of the type $[(phosphinine)CuBr]_2$, which show a rare distorted trigonal planar coordination environment at the Cu(I) centers. In fact, the core of **8** in the solid-state shows a butterfly structure, while the one in **9** and **10** each display each a planar, P–Cu_2Br_2–P moiety. Upon reaction of the 3-*N*,*N*-dimethylaminophosphinines with $AuCl \cdot S(CH_3)_2$, mononuclear phosphinine-Au(I)-complexes were formed quantitatively. The novel phosphinines are prone to post-synthetic ligand modification, as they can easily be protonated exclusively at the nitrogen atom, while protodesilylation occurs in acetonitrile at higher temperature. The formed phosphinine-based hydrochloride salts react with $CuCl \cdot SMe_2$ to form a rare Cu(I)-complex with a Cu_4Cl_4-core, that contains two pairs of differently coordinating phosphinine ligands.

Experimental Section

General Remarks

All reactions were performed under argon in oven-dried glassware using modified Schlenk techniques unless otherwise stated. All common solvents and chemicals were commercially available and were used without further purification. All dry or deoxygenated solvents were prepared using standard techniques or were used from MBraun solvent purification system. *N,N*-dimethyl-2-phenylethyn-1-amine, 1,3,2-diazaphosphinines, **6**, **13** and **14** were prepared according to literature.[5,12,19] The ^{1}H, ^{19}F, ^{13}C{^{1}H}, ^{31}P{^{1}H} and ^{31}P NMR spectra were recorded on a *JEOL* ECX400 (400 MHz) spectrometer or a Bruker Avance 600 (600 MHz) spectrometer and all chemical shifts are reported relative to the residual resonance in the deuterated solvents. The HRMS ESI mass spectra were measured on an Agilent 6210 ESI-TOF. Low-temperature x-ray diffractometry was performed on a Bruker-AXS X8 Kappa Duo diffractometer with *IμS* micro-sources, performing ϕ-and ω-scans. Data was collected using a Photon 2 CPAD detector with Mo K_α radiation (λ = 0.71073 Å) or Cu K_α radiation (λ = 1.5406 Å). The structures were solved by dual-space methods using SHELXT[20] and refined against F^2 on all data by full-matrix least squares with SHELXL-2017[21] following established refinement strategies[22]. The program Olex2[23] was also used to aid in the refinement. All non-hydrogen atoms were refined anisotropically. All hydrogen atoms were included into the model at geometrically calculated positions and refined using a riding model. The isotropic displacement parameters of all hydrogen atoms were fixed to 1.2 times the *U*-value of the atoms they are linked to (1.5 times for methyl groups). Details of the data quality and a summary of the residual values of the refinements are listed in Table S1 below. Tables S2, S4, S6, S8, S10, S12, S14 and S16 give all bond lengths for the structures and S3, S5, S7, S9, S11, S13, S15 and S17 give all angles for the structures. Supplementary crystallographic data for **5**, **7**–**12** and **15** can be found in the CCDC with the following deposit numbers CCDC 2214696 (**5**), 2214697 (**7**), 2214698 (**8**), 2214699 (**9**), 2214700 (**10**), 2214701 (**11**) and 2214702 (**12**), 2217680 (**15**). These data can be obtained free of charge from www.ccdc.cam.ac.uk/data_request/cif.

General method for the synthesis of compounds 5 and 7. Compounds **5** and **7** were prepared analogously to **6**[12]: 1 equiv. of the (trimethylsilyl)acetylene derivative (2.0 mmol) was added to a solution of 1,3,2-diazaphosphinine (2.0 mmol) in toluene (15 mL). The mixture was heated to T = 70 °C for 5 hours. The complete formation of the 1,2-monoazaphosphinine was monitored by ^{31}P NMR spectroscopy and all volatiles were removed under vacuum. The reaction of residual solids with 2 equiv. of *N,N*-dimethyl-2-phenylethyn-1-amine (0.58 g, 4 mmol) in 15 mL toluene was heated to T = 90 °C (for compound **5**, T = 80 °C) overnight. At the end of reaction, the solution was removed under vacuum and the product was purified by column chromatography on silica with *n*-hexane/ethyl acetate as eluent (9:1). For **5**: (Trimethylsilyl)acetylene derivative: (trimethylsilyl)acetylene (0.20 g, 2.0 mmol), product yield: 477 mg, 1.7 mmol, 83 %. **^{1}H NMR (600 MHz, *CDCl$_3$*)** δ 7.96 (t, ^{3}J(H,P) = 10.8 Hz, 1H, C_5H_2P), 7.53 (d, J = 7.6 Hz, 2H, *-Ph*), 7.40 (t, J = 7.6 Hz, 2H, *-Ph*), 7.29 (t, J = 7.6 Hz, 1H, *-Ph*), 7.15 (d, ^{4}J(H,P) = 8.7 Hz, 1H, C_5H_2P), 2.63 (s, 6H, *-NMe$_2$*), 0.36 (s, 9H, *-TMS*) ppm; **^{13}C{^{1}H} NMR (151 MHz, *CDCl$_3$*)** δ 159.1 (d, ^{1}J(C,P) = 58.6 Hz), 158.3 (d, ^{1}J(C,P) = 72.1 Hz), 155.0 (d, ^{2}J(C,P) = 10.8 Hz), 143.5 (d, ^{2}J(C,P) = 23.3 Hz), 138.9 (d, ^{2}J(C,P) = 12.7 Hz), 128.7 (d, ^{3}J(C,P) = 10.6 Hz), 128.5 (s, *C11*), 126.6 (s, *C10*), 119.5 (d, ^{3}J(C,P) = 17.6 Hz), 42.8 (s), 0.2 (d, ^{3}J(C,P) = 5.9 Hz) ppm; **^{31}P{^{1}H} NMR (162 MHz, *CD$_2$Cl$_2$*)** δ 238.0 ppm; **HR-ESI MS** (*m/z*): 288.1461 g/mol (calculated: 288.1332 g/mol) [M][H]$^+$. For **7**: (Trimethylsilyl)acetylene derivative: 1-phenyl-2-trimethylsilylacetylene (0.35 g, 2.0 mmol), yield: 589 mg, 1.6 mmol, 81 %. **^{1}H NMR (600 MHz, *CD$_2$Cl$_2$*)** δ 7.54 (d, J = 8.2, 1.2 Hz, 2H, *-Ph*), 7.45–7.38 (m, 5H, *-Ph*), 7.34 (dd, J = 7.7, 1.7 Hz, 2H, *-Ph*), 7.30 (t, J = 7.4, 1.3 Hz, 1H, *-Ph*), 6.95 (d, J = 1.5 Hz, 1H, C_5HP), 2.61 (s, 6H, *-NMe$_2$*), 0.04 (d, J = 1.5 Hz, 9H, *-TMS*) ppm; **^{13}C{^{1}H} NMR (151 MHz, *CD$_2$Cl$_2$*)** δ 157.5 (s), 155.8 (d, ^{1}J(C,P) = 60.6 Hz), 155.8 (d, ^{1}J(C,P) = 83.1 Hz), 154.7 (d, ^{2}J(C,P) = 9.7 Hz), 146.1 (d, ^{2}J(C,P) = 12.8 Hz), 143.0 (d, ^{2}J(C,P) = 24.6 Hz), 129.0(s), 128.8 (d, ^{3}J(C,P) = 10.6 Hz), 128.4 (s), 127.8 (s), 127.3 (s), 126.6 (s), 122.4 (d, ^{3}J(C,P) = 14.3 Hz), 42.6 (s), 1.8 (d, ^{3}J(C,P) = 10.1 Hz) ppm; **^{31}P{^{1}H} NMR (243 MHz, *CD$_2$Cl$_2$*)** δ 245.0 ppm.

General method for the synthesis of complexes 8–10: Phosphinine (0.1 mmol) and copper(I) bromide dimethyl sulfide complex (21 mg, 0.1 mmol) were added in Schlenk flask and 4 mL THF solvent was added to the flask. The solvent was removed under vacuum after the mixture was stirred at room temperature for overnight. Single crystals, suitable for X-ray diffraction, were obtained from a MeCN solution of the complex by slow evaporation of the solvent in the glovebox. For **8**: Phosphinine **5** (29 mg, 0.1 mmol), yield: 40 mg, 0.047 mmol, 93 %. **^{1}H NMR (600 MHz, *CD$_3$CN*)** δ 7.98 (dd, ^{3}J(H,P) = 18.9, J = 9.1 Hz, 2H, C_5H_2P), 7.50 (d, J = 7.5 Hz, 4H, *-Ph*), 7.42 (t, J = 7.6 Hz, 4H,*-Ph*), 7.33 (t, J = 7.1 Hz, 2H, *-Ph*), 7.19 (dd, ^{4}J(H,P) = 10.2, 2.6 Hz, 2H, C_5H_2P), 2.58 (s, 12H, *-NMe$_2$*), 0.38 (s, 18H, *-TMS*) ppm; **^{13}C{^{1}H} NMR (151 MHz, *CD$_3$CN*)** δ 157.5 (d, ^{2}J(C,P) = 8.1 Hz), 152.3 (d, ^{1}J(C,P) = 20.1 Hz), 150.0 (d, ^{1}J(C,P) = 44.1 Hz), 143.0 (d, ^{2}J(C,P) = 18.2 Hz), 141.5 (d, ^{2}J(C,P) = 15.2 Hz), 130.1 (d, ^{3}J(C,P) = 10.7 Hz), 129.5 (s), 128.0 (s), 120.0 (d, ^{3}J(C,P) = 23.1 Hz), 42.9 (s), 0.4 (d, ^{3}J(C,P) = 4.9 Hz) ppm; **^{31}P{^{1}H} NMR (243 MHz, *CD$_3$CN*)** δ 203 ppm; **HR-ESI MS** (*m/z*): 860.1451 g/mol (calculated: 859.9452 g/mol) [M][H]$^+$. For **9**: Phosphinine **6** (30 mg, 0.1 mmol), yield: 41 mg, 0.047 mmol, 93 %. **^{1}H NMR (600 MHz, *CD$_3$CN*)** δ 7.49 (d, J = 7.6 Hz, 4H, *-Ph*), 7.40 (t, J = 7.5 Hz, 4H, *-Ph*), 7.31 (t, J = 7.5 Hz, 2H, *-Ph*), 7.02 (s, 2H, C_5HP), 2.59 (d, J = 2.0 Hz, 18H, *3-NMe$_2$ & 5-Me*), 0.42 (s, 18H, *-TMS*) ppm; **^{31}P{^{1}H} NMR (162 MHz, *CD$_3$CN*)** δ 223 ppm; **HR-ESI MS** (*m/z*): 888.1794 g/mol (calculated: 887.9765 g/mol) [M][H]$^+$; A suitable ^{13}C{^{1}H} spectrum could not be obtained due to the poor solubility of this compound in organic solvents. For **10**: Phosphinine **7** (36 mg, 0.1 mmol), yield: 45 mg, 0.044 mmol, 88 %. **^{1}H NMR (600 MHz, *CD$_3$CN*)** δ 7.55 (dt, J = 8.1, 1.3 Hz, 4H, *-Ph*), 7.47–7.41 (m, 10H, *-Ph*), 7.37–7.32 (m, 6H, *-Ph*), 6.95 (d, ^{4}J(H,P) = 2.3 Hz, 2H, C_5HP), 2.60 (s, 12H, *3-NMe$_2$*), 0.05 (d, J = 1.4 Hz, 18H, *-TMS*) ppm; **^{13}C{^{1}H} NMR (151 MHz, *CD$_3$CN*)** δ 155.9 (s), 155.7 (d, ^{2}J(C,P) = 13.7 Hz), 154.7 (d, ^{2}J(C,P) = 7.5 C Hz) 149.8 (d, ^{1}J(C,P) = 63.6 Hz), 145.7 (s), 142.3 (d, ^{1}J(C,P) = 21.8 Hz), 130.7 (s), 129.0 (s), 128.7 (s), 128.0 (s), 127.6 (s), 127.0 (s), 122.0 (d, ^{3}J(C,P) = 17.3 Hz), 41.9 (s), 1.5 (d, ^{3}J(C,P) = 9.2 Hz) ppm; **^{31}P{^{1}H} NMR (243 MHz, *CD$_3$CN*)** δ 224 ppm; **HR-ESI MS** (*m/z*): 1012.2001 g/mol (calculated: 1012.0078 g/mol) [M][H]$^+$.

General method for the synthesis of complexes 11–12: Phosphinine (0.1 mmol) and chloro(dimethylsulfide)gold(I) (30 mg, 0.1 mmol) were added in a Schlenk flask and 3 mL THF solvent was added to the flask. The solvent was removed under vacuum after the mixture was stirred at room temperature for overnight. Crystallization was achieved by layering hexanes onto a MeCN solution of the complex in a freezer at T = −30 °C. For **11**: Phosphinine **5** (29 mg, 0.1 mmol), yield: 47 mg, 0.09 mmol, 90 %.**^{1}H NMR (600 MHz, *CD$_3$CN*)** δ 8.11 (ddd, ^{3}J(H,P) = 34.1, 9.3, 1.6 Hz, 1H, C_5H_2P), 7.52 (d, J = 9.1 Hz, 2H, *-Ph*), 7.46 (t, J = 7.4 Hz, 2H, *1-Ph*), 7.42 (t, J = 4.8 Hz, 1H, *-Ph*), 7.23 (dd, ^{4}J(H,P) = 9.8, 6.5 Hz, 1H, C_5H_2P), 2.65 (d, J = 1.6 Hz, 6H, *-NMe$_2$*), 0.45 (d, J = 1.7 Hz, 9H, *-TMS*) ppm; **^{13}C{^{1}H} NMR (151 MHz, *CD$_3$CN*)** δ 159.3 (s), 145.0 (d, ^{1}J(C,P) = 38.6 Hz), 143.2 (d, ^{1}J(C,P) = 16.6 Hz), 142.4 (s), 140.5 (d, ^{2}J(C,P) = 10.2 Hz), 130.7 (d, ^{3}J(C,P) = 10.9 Hz), 130.0 (s), 128.9 (s), 120.1 (d, ^{3}J(C,P) = 31.7 Hz), 42.8 (s), 0.7 (d, ^{3}J(C,P) = 4.3 Hz); **^{31}P{^{1}H} NMR (243 MHz, *CD$_3$CN*)** δ 193 ppm; **HR-ESI MS** (*m/z*): 542.0506 g/mol (calculated: 542.0549 g/mol) [M]Na$^+$. For **12**: Phosphinine **7** (36 mg, 0.1 mmol), product yield: 54 mg, 0.09 mmol, 90 %. **^{1}H NMR (600 MHz, *CD$_3$CN*)** δ 7.57–7.53 (m, 2H, *-Ph*), 7.49–7.45 (m, 6H, *-Ph*),

7.39–7.35 (m, 2H, *-Ph*), 6.96 (d, J = 4.0 Hz, 1H, C_5HP), 2.64 (d, J = 0.8 Hz, 6H, *-NMe$_2$*), 0.14 (dd, J = 1.6, 0.9 Hz, 9H, *-TMS*) ppm; **^{13}C{^{1}H} NMR (151 MHz, *CD$_3$CN*)** δ 157.4 (d, ^1J(C,P) = 53.4 Hz), 157.4 (d, ^1J(C,P) = 67.7 Hz), 157.3 (s), 155.9 (s), 145.2 (d, ^2J(C,P) = 13.6 Hz), 130.0 (d, ^2J(C,P) = 10.8 Hz), 128.8 (s), 128.3 (s), 128.2 (d, ^3J(C,P) = 7.8 Hz), 128.0 (s), 128.0 (s), 127.6 (s), 121.6 (d, ^3J(C,P) = 26.7 Hz), 41.9 (s), 2.3 (d, ^3J(C,P) = 5.8 Hz) ppm; **^{31}P{^{1}H} NMR (243 MHz, *CD$_3$CN*)** δ 205 ppm; **HR-ESI MS** (*m/z*): 618.0819 g/mol (calculated: 618.0783 g/mol) [M]Na$^+$.

For the synthesis of complex 15: Protonated phosphinine **14** (27 mg, 0.1 mmol) was dissolved in DCM (3 mL) at room temperature and copper(I) chloride dimethyl sulfide complex (16 mg, 0.1 mmol, 1 eq.) was added to the Schlenk flask. The reaction was stirred at room temperature overnight before filtering the orange solution through Celite. All volatiles of the filtrate were removed under vacuum yielding **15** as an orange solid. Yield: 92% (30.2 mg, 0.023 mmol). Crystals of **15** suitable for single crystal X-ray diffraction were obtained from a mixture of THF (1 mL) and *n*-hexane (1 mL) in a freezer at T = −30 °C. **^{1}H NMR (600 MHz, THF-*d$_8$*)** δ 7.70 (d, $^2J_{H,P}$ = 29.9 Hz, 1H, C_5H_2P), 7.51 (d, J = 7.5 Hz, 2H, *Ph*), 7.22 (t, J = 7.5 Hz, 2H, *Ph*), 7.12 (t, J = 7.4 Hz, 1H, *Ph*), 6.96 (d, $^4J_{H,P}$ = 3.9 Hz, 1H, C_5H_2P), 2.54 (s, 6H, N*Me$_2$*), 2.42 (s, 3H, CH_3) ppm; **^{13}C{^{1}H} NMR (151 MHz, THF-*d$_8$*)** δ 157.9 (d, ^2J(C,P) = 9.0 Hz), 147.6 (s), 147.3 (d, ^2J(C,P) = 15.4 Hz), 141.6 (d, ^1J(C,P) = 17.2 Hz), 137.9 (s), 130.5 (d, ^2J(C,P) = 10.9 Hz), 129.3 (s), 127.5 (s), 121.8 (d, ^1J(C,P) = 19.2 Hz), 43.2 (s), 26.0 (s) ppm; **^{31}P{^{1}H} NMR (162 MHz, THF-*d$_8$*)** δ 173 ppm.

Acknowledgements

The authors express their sincere thanks to Freie Universität Berlin and the China Scholarship Council for funding. Open Access funding enabled and organized by Projekt DEAL.

Conflict of Interest

The authors declare no conflict of interest.

Data Availability Statement

The data that support the findings of this study are available in the supplementary material of this article.

Keywords: Au(I) Complexes · Coordination Chemistry · Cu(I) Complexes · DFT Calculations · Phosphinine

[1] N. T. Coles, A. S. Abels, J. Leitl, R. Wolf, H. Grützmacher, C. Müller, *Coord. Chem. Rev.* **2021**, *433*, 213729.
[2] G. Märkl, *Angew. Chem. Int. Ed. Engl.* **1966**, *5*, 846–847.
[3] A. J. Ashe III, *J. Am. Chem. Soc.* **1971**, *93*, 3293–3295.
[4] W. Rösch, M. Regitz, *Z. Naturforsch. B* **1986**, *41*, 931–934.
[5] a) N. Avarvari, P. Le Floch, F. Mathey, *J. Am. Chem. Soc.* **1996**, *118*, 11978–11979; b) N. Avarvari, P. Le Floch, L. Ricard, F. Mathey, *Organometallics* **1997**, *16*, 4089–4098.
[6] a) R. J. Newland, M. F. Wyatt, R. L. Wingard, S. M. Mansell, *Dalton Trans.* **2017**, *46*, 6172–6176; b) R. J. Newland, M. P. Delve, R. L. Wingad, S. M. Mansell, *New J. Chem.* **2018**, *42*, 19625–19636; c) P. A. Cleaves, S. M. Mansell, *Organometallics* **2019**, *38*, 1595–1605.
[7] a) K. Nakajima, S. Takata, K. Sakata, Y. Nishibayashi, *Angew. Chem.* **2015**, *127*, 7707–7711; *Angew. Chem. Int. Ed.* **2015**, *54*, 7597–7601; b) T. Gläsel, H. Jiao, M. Hapke, *ACS Catal.* **2021**, *11*, 13434–13444.
[8] a) M. H. Habicht, F. Wossidlo, T. Bens, E. A. Pidko, C. Müller, *Chem. Eur. J.* **2018**, *24*, 944–952; b) J. Lin, F. Wossidlo, N. T. Coles, M. Weber, S. Steinhauer, T. Böttcher, C. Müller, *Chem. Eur. J.* **2021**, *28*, e202104135; c) F. Wossidlo, D. S. Frost, J. Lin, N. T. Coles, K. Klimov, M. Weber, T. Böttcher, C. Müller, *Chem. Eur. J.* **2021**, *27*, 12788–12795; d) L. Fischer, F. Wossidlo, D. S. Frost, N. T. Coles, S. Steinhauer, S. Riedel, C. Müller, *Chem. Commun.* **2021**, *57*, 9522–9525.
[9] Y. Mao, K. M. H. Lim, Y. Li, R. Ganguly, F. Mathey, *Organometallics* **2013**, *32*, 3562–3565.
[10] Y. Hou, Z. Li, Y. Li, P. Liu, C.-Y. Su, F. Puschmann, H. Grützmacher, *Chem. Sci.* **2019**, *10*, 3168–3180.
[11] S. Giese, K. Klimov, A. Mikeházi, Z. Kelemen, D. S. Frost, S. Steinhauer, P. Müller, L. Nyulászi, C. Müller, *Angew. Chem. Int. Ed.* **2021**, *60*, 3581–3586; *Angew. Chem.* **2021**, *133*, 3625–3630.
[12] J. Lin, N. T. Coles, L. Dettling, L. Steiner, J. F. Witte, B. Paulus, C. Müller, *Chem. Eur. J.* **2022**, e202203406.
[13] P. Roesch, J. R. Nitsch, M. Lutz, J. Wiecko, A. Steffen, C. Müller, *Inorg. Chem.* **2014**, *53*, 9855–9859.
[14] X. Chen, Z. Li, F. Yanan, H. Grützmacher, *Eur. J. Inorg. Chem.* **2016**, *2016*, 633–638.
[15] H. Kanter, K. Dimroth, *Tetrahedron Lett.* **1975**, *16*, 541–544.
[16] M. Shiotsuka, T. Tanamachi, T. Urakawa, M. Munakata, Y. Matsuda, *J. Supramol. Chem.* **2002**, *2*, 211–217.
[17] N. Mézailles, P. Le Floch, K. Waschbüsch, L. Ricard, F. Mathey, C. P. Kubiak, *J. Organomet. Chem.* **1997**, *541*, 277–283.
[18] a) J. Moussa, L. M. Chamoreau, H. Amouri, *RSC Adv.* **2014**, *4*, 11539–11542; b) J. Stott, C. Bruhn, U. Siemeling, *Z. Naturforsch. B* **2013**, *68*, 853–859; c) M. Rigo, L. Hettmanczyk, F. J. L. Heutz, S. Hohloch, M. Lutz, B. Sarkar, C. Müller, *Dalton Trans.* **2017**, *46*, 86–95; d) N. Mézailles, L. Ricard, F. Mathey, P. Floch, *Eur. J. Inorg. Chem.* **1999**, *1999*, 2233–2241; e) M. Rigo, E. R. M. Habraken, K. Bhattacharyya, M. Weber, A. W. Ehlers, N. Mézailles, J. C. Slootweg, C. Müller, *Chem. Eur. J.* **2019**, *25*, 8769–8779.
[19] L. Hong, S. Ahles, M. A. Strauss, C. Logemann, H. A. Wegner, *Org. Chem. Front.* **2017**, *4*, 871–875.
[20] G. M. Sheldrick, *Acta Crystallogr. Sect. A* **2015**, *71*, 3–8.
[21] G. M. Sheldrick, *Acta Crystallogr. Sect. C* **2015**, *71*, 3–8.
[22] P. Müller, *Crystallogr. Rev.* **2009**, *15*, 57–83.
[23] O. V. Dolomanov, L. J. Bourhis, R. J. Gildea, J. A. K. Howard, H. Puschmann, *J. Appl. Crystallogr.* **2009**, *42*, 339–341.

Manuscript received: November 16, 2022
Revised manuscript received: December 12, 2022
Accepted manuscript online: December 12, 2022

